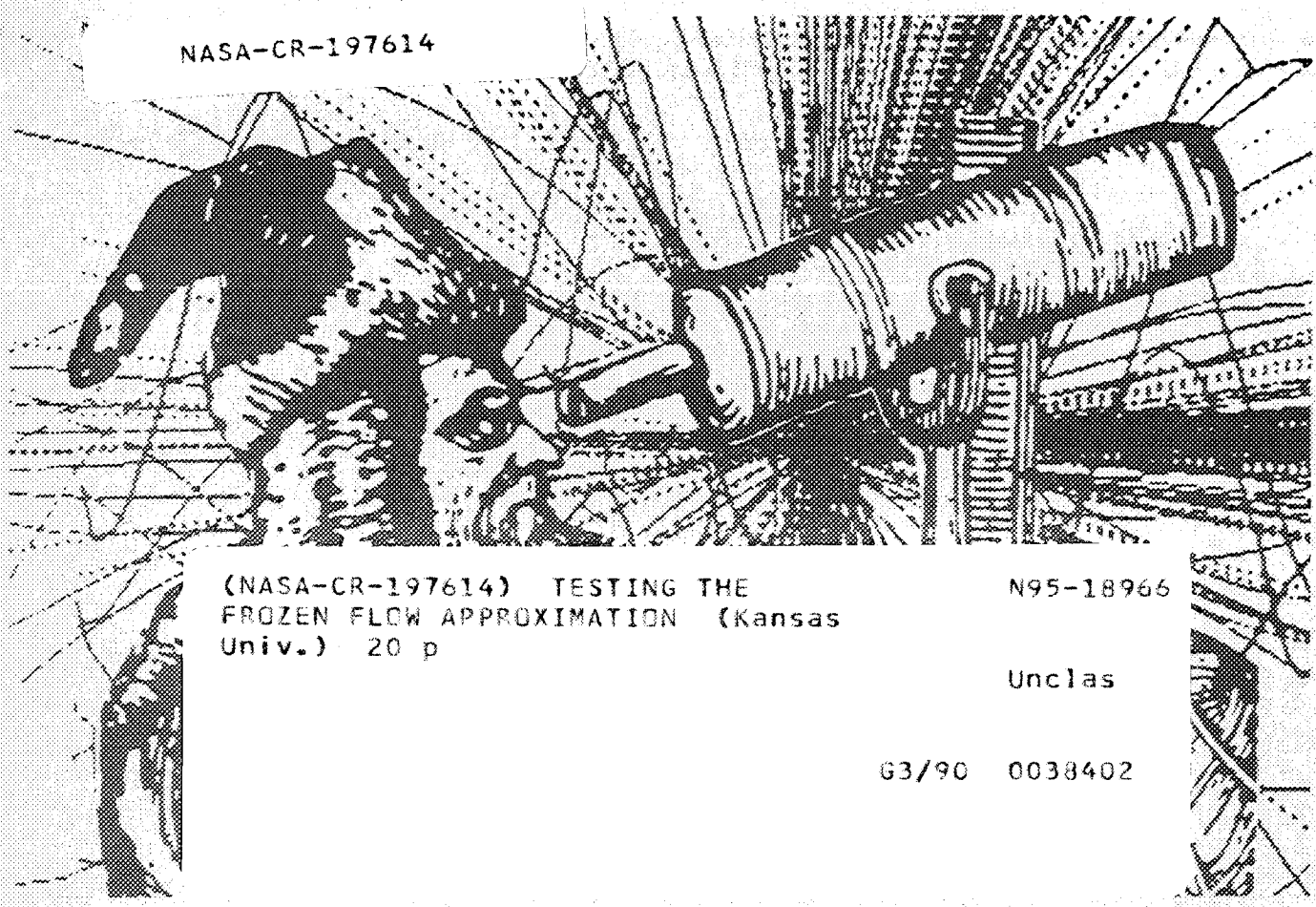

THE UNIVERSITY OF KANSAS

Testing the Frozen Flow Approximation

Francesco Lucchin[1], **Sabino Matarrese**[2], **Adrian L. Melott**[3] and **Lauro Moscardini**[1]
[1] Dipartimento di Astronomia
Università di Padova, Italy
[2] Dipartimento di Fisica "G. Galilei",
Università di Padova, Italy
[3] Department of Physics and Astronomy,
University of Kansas

Department of Physics and Astronomy

Lawrence, Kansas 66045

Testing the Frozen–Flow Approximation

Adrian L. Melott,[1] **Francesco Lucchin,**[2] **Sabino Matarrese,**[3] and **Lauro Moscardini**[2]

1. Department of Physics and Astronomy, University of Kansas, Lawrence, Kansas 60645 USA

2. Dipartimento di Astronomia, Università di Padova, vicolo dell'Osservatorio 5, I–35122 Padova, Italy

3. Dipartimento di Fisica "G. Galilei", Università di Padova, via Marzolo 8, I–35131 Padova, Italy

Abstract: We investigate the accuracy of the frozen–flow approximation (FFA), recently proposed by Matarrese et al. (1992), for following the nonlinear evolution of cosmological density fluctuations under gravitational instability. We compare a number of statistics between results of the FFA and nbody simulations, including those used by Melott, Pellman & Shandarin (1993) to test the Zel'dovich approximation. The FFA performs reasonably well in a statistical sense, e.g. in reproducing the counts–in–cell distribution, at small scales, but it does poorly in the crosscorrelation with nbody which means it is generally not moving mass to the right place, especially in models with high small–scale power.

1. INTRODUCTION

Gravitational instability is the dominant theory of how structure grew in the universe. The primary tools for understanding this process have been linear perturbation theory, the "Zel'dovich approximation", and direct numerical integration, usually called "nbody simulations." For a review see Shandarin & Zel'dovich (1989).

Choosing the best approximation for a given use is extremely important, as approximations often form the basis for semianalytic arguments about galaxy and/or large–scale structure formation, and are often used to provide initial conditions or boundary conditions for nbody simulations.

The Zel'dovich (1970) approximation (ZA) was originally applied to so–called "pancake" models, in which high–frequency modes are missing from the initial mass density fluctuation spectrum. Beginning in Melott et al. (1983), evidence began to appear that pancake–like structures might arise in models without such damped initial conditions. More recently, ZA has been used to follow a variety of models into the quasilinear regime. A variety of improvements on it have been proposed.

Coles, Melott & Shandarin (1993) (hereafter CMS) began systematic and quantitative testing of some dynamical approximations, emphasizing the use of a variety of initial conditions, and using crosscorrelation analysis to test dynamics. Melott et al. (1993) (hereafter MPS) did a detailed study of the approximation CMS had determined to be the best, finding that it could be considerably improved. The result was the truncated Zel'dovich approximation (TZA), which is nothing more than the ZA with a specific filtering of initial conditions. We used here the same nbody simulations and the same comparison methods used in these two papers and in this work report results on the frozen–flow approximation (FFA) as described in Matarrese et al. (1992) (hereafter MLMS).

The plan of the paper is as follows. In section 2 we describe this approximation, as well as the Zel'dovich approximation to which it is related. In section 3 we define our main tool to compare the dynamics of different approximations and nbody simulations: the crosscorrelation analysis. Section 4 presents the results of this analysis applied to FFA and TZA vs. nbody, as well as some other statistics applied to the particle distributions. A final discussion section concludes our paper.

2. FROZEN–FLOW APPROXIMATION

The standard Newtonian equations for the evolution of collisionless matter in the universe can be rewritten in terms of suitably rescaled variables and in comoving coordinates. In particular, it is sometimes convenient to use as time variable the growth factor of linear perturbations, which in a flat, matter dominated model, coincides with the expansion factor $a(t) = a_0(t/t_0)^{2/3}$ (a subscript 0 will be used for the "initial time" t_0). The Euler equations read

$$\frac{d\mathbf{u}}{da} + \frac{3}{2a}\mathbf{u} = -\frac{3}{2a}\nabla\varphi, \tag{1}$$

where $\mathbf{u} \equiv d\mathbf{x}/da$ is a rescaled comoving peculiar velocity field and the symbol $\frac{d}{da}$ stands for the total (convective) derivative $\frac{d}{da} = \frac{\partial}{\partial a} + \mathbf{u}\cdot\nabla$. The continuity equation can be

written in terms of the comoving matter density $\eta(\mathbf{x},t) \equiv \varrho(\mathbf{x},t)$ density at t_0)

$$\frac{d\eta}{da} + \eta \nabla \cdot \mathbf{u} = 0, \tag{2}$$

while the rescaled local gravitational potential $\varphi \equiv (3t_0^2/2a_0^3)\phi(\mathbf{x},t)$ is determined by local density inhomogeneities $\delta(\mathbf{x},t) \equiv \eta(\mathbf{x},t) - 1$ through Poisson's equation

$$\nabla^2 \varphi = \frac{\delta}{a}. \tag{3}$$

We restrict our analysis to irrotational flow.

The Zel'dovich approximation, in these variables, corresponds to the ansatz $\mathbf{u} = -\nabla\varphi$, as suggested by linear theory. In this case the Euler and continuity equations decouple from Poisson's one, and the system describes inertial motion of particles with initial velocity field impressed by local gravity, as implied by the growing mode of linear perturbation theory: $\mathbf{u}_{ZA}(\mathbf{x},\tau) = -\nabla_{\mathbf{q}}\varphi_0(\mathbf{q})$, where $\mathbf{q}$ is the initial (Lagrangian) position and $\tau \equiv a - a_0$. It follows that particles move along straight trajectories

$$\mathbf{x}(\mathbf{q},\tau) = \mathbf{q} - \tau \nabla_{\mathbf{q}}\varphi_0(\mathbf{q}). \tag{4}$$

The frozen–flow approximation can be defined as the solution of the linearized Euler equations, where in the r.h.s. the growing mode of the linear gravitational force is assumed, $\mathbf{u}_{FFA}(\mathbf{x},\tau) = \mathbf{u}_0(\mathbf{x}) = -\nabla_{\mathbf{x}}\varphi_0(\mathbf{x})$, plus a negligible decaying mode. In this approximation the peculiar velocity field $\mathbf{u}(\mathbf{x},a)$ is *frozen* at each point to its initial value, that is

$$\frac{\partial \mathbf{u}}{\partial \tau} = 0, \tag{5}$$

which is just the condition for steady flow. The above equation, together with the continuity equation, define FFA. Particle trajectories in FFA are described by the integral equation

$$\mathbf{x}(\mathbf{q},\tau) = \mathbf{q} - \int_0^\tau d\tau' \nabla_{\mathbf{x}}\varphi_0[\mathbf{x}(\mathbf{q},\tau')]. \tag{6}$$

Particles update their velocity at each infinitesimal step to the local value of the linear velocity field, without any memory of their previous motion, i.e. without *inertia*. Streamlines are then frozen to their initial shape and multi–stream regions cannot form. A particle moving according to FFA has zero component of the velocity in a place where the same component of the initial gravitational force is zero, it will then slow down its motion in that direction while approaching that place. Unlike the Zel'dovich approximation, these particles move along curved paths: once they come close to a pancake configuration they curve their trajectories, moving almost parallel to it, and trying to reach the position of the next filament. Again they cannot cross it, so they modify their motion, while approaching it, to finally fall, for $\tau \to \infty$, into the knots corresponding to the minima of the initial gravitational potential. This type of dynamics implies an artificial thickening of particles around pancakes, filaments and knots, which mimics the gravitational clustering around

these structures (though these configurations do not necessarily occur in the right Eulerian locations, nor they necessarily involve the right Lagrangian fluid elements). In assuming that the velocity potential is linearly related at any time to the local value of the initial gravitational potential, FFA disregards the non–linear effects caused by the back–reaction of the evolving mass density on the peculiar velocity field itself (via the non–linear evolution of the gravitational potential). This implies that a number of physical processes such as merging of pancakes, fragmentation and disruption of low–density bridges, are totally absent in the FFA dynamics. Unlike the velocity field, the FFA density field is non–locally determined by the initial fluctuations, via the continuity equation; this is clearly shown by the following analytic expression

$$1 + \delta_{FFA}(\mathbf{x}, \tau) = \exp \int_0^\tau d\tau' \delta_+[\mathbf{x}(\mathbf{q}, \tau')] \tag{7}$$

(where $\delta_+ \equiv \delta_0/a_0$). Brainerd, Scherrer & Villumsen (1993) have recently shown that a similar formula also applies if one uses a different approximation (called LEP: linear evolution of potential), consisting in "freezing" the gravitational rather than the velocity potential [see also the equivalent "frozen–potential" approach by Bagla & Padmanabhan (1993)]. This approach shows many features in common to FFA, although multi–stream regions do occur in this case.

Numerical implementation of FFA is straightforward (for a more technical discussion, see MLMS) and involves small computing time: roughly speaking, FFA consists of a multi–step Zel'dovich approximation, and very few steps are required to follow the entire evolution. MLMS applied FFA to follow the evolution of structures in the standard CDM model, and found that it gives a fairly accurate representation of the density pattern from a resolution scale of $\sim$ 500 km s^{-1}, while the two–point correlation function fits quite well the true non–linear result on even smaller scales. Further connections of FFA and ZA can be found, based on the Hamilton–Jacobi approach to the non–linear dynamics of collisionless matter. These, as well as other features of FFA, will be discussed elsewhere.

3. TESTING COMPARISONS

We will use a group of nbody simulations, described in considerable detail elsewhere (Melott & Shandarin 1993, hereafter MS). MS used an ensemble of simulations to get average values for a number of quantities and determine which are the most stable statistics. However, such ensembles are not necessary to unearth systematic effects when everything else is held constant, as verified by CMS. Here as in MPS, we use a subset of the ensemble: four simulations with initial power–law density fluctuation power spectra

$$P(k) = \mid \delta(k) \mid^2 \propto k^n, \tag{8}$$

with values $n = 1, 0, -1$, and -2. The case $n = -3$ is basically limited by boundary conditions rather than the details of time evolution, and so is not very interesting to follow. These Particle–Mesh nbody simulations have 128^3 particles on a 128^3 mesh, and are followed from very low amplitudes until the clustering is so advanced that the absence of modes outside the box begins to be a problem; this means an expansion factor of as

much as 5000. All are done in an $\Omega = 1$ (Einstein–De Sitter) background to preserve self–similarity as much as possible.

Stages are defined by the nonlinearity scale k_{nl}:

$$a^2(t) \int_0^{k_{nl}} P(k) d^3k = 1, \tag{9}$$

where P is the power in the initial conditions. This scale k_{nl} is the one which is, according to linear theory, going nonlinear. We study here primarily the stage $k_{nl} = 8k_f$ where k_f is the fundamental mode of the box, but also crosschecked our results for consistency with $k_{nl} = 4k_f$.

We will check a number of statistics for agreement between the models: the power spectra, agreement of phases of Fourier components, the mass density distribution, and its variance and skewness. We will examine the visual appearance. But because we are testing dynamical approximations and not toy models, we must also determine if mass has been moved to the right place; statistical agreement is not enough.

Following CMS and MPS, we study the cross–correlation coefficient

$$S = \frac{\langle \delta_1 \delta_2 \rangle}{\sigma_1 \sigma_2}, \tag{10}$$

where $\sigma_i = \langle \delta_i^2 \rangle^{1/2}$ and δ_1, δ_2 are the pixellized density contrasts in the simulation and nbody distribution, respectively. Of course $\mid S \mid \leq 1$, and $S = +1$ implies $\delta_1 = C\delta_2$ where C is a constant.

This statistic has one overwhelming advantage over any other we can apply to the mass distribution: as it approaches unity, *all* other statistics must come into agreement. (Unless $S = 1$ but $C \neq 1$; this is nearly impossible here due to the way skewness grows with gravity.)

One possible problem with this approach is that an approximation might create the right sort of condensations, but put them in slightly the wrong place. The density peaks would miss each other and produce a small S. For this reason as in CMS/MPS we also study smoothed fields. We smooth both δ_1 and δ_2 by convolution with the same Gaussian $e^{-R^2/2R_G^2}$ and plot the results as a function of σ_2 after smoothing. Thus, in the case above, a large value of S would appear with modest smoothing indicating good agreement of the smoothed fields.

Brainerd et al. (1993) have criticized this approach. They studied evolution based on LEP and on the ordinary ZA, and compared with an nbody simulation of Cold Dark Matter. Both the nbody and the LEP produced small condensations and ZA diffuse condensations in the same general region. Thus in some sense nbody and LEP are more similar. Yet they found the unsmoothed crosscorrelation was higher between nbody and ZA, and concluded that the value of crosscorrelation was questionable for unsmoothed fields.

We disagree. In this test, LEP was penalized because it "claimed" accuracy in excess of what it had. Condensations had errors of position large compared to their diameters. On the scale of the diameters the dynamics were wrong, as can be seen by visually examining

their plots. On the other hand, the more conservative ZA represented its uncertainty by creating diffuse condensations, which do include the analogous region in the nbody simulation, and produced a stronger crosscorrelation. It is possible that LEP could crosscorrelate much better than ZA or even TZA (see below) if examined with modest smoothing. The pattern on medium scales appeared quite good.

The strategy in this paper, CMS, MPS, and near future work is to compare a series of approximations in the same way. Thus we need to compare the performance of FFA with some other approximation. The best that has emerged to date is the Truncated Zel'dovich Approximation (TZA) as described by MPS. Applying this approximation is simple, but results in a dramatic improvement over ZA. One convolves the initial density field (still linear) with a Gaussian $e^{-k^2/2k_G^2}$. The best choice value lies in the range $k_{nl} \leq k_G \leq 1.5k_{nl}$, depending on the spectrum (MPS). It may seem paradoxical, but this smoothing of the initial conditions produces a less smooth approximation in the nonlinear regime. It focuses pancakes where the mass is, removing highly nonlinear modes which promote shell crossing and diffuseness. As an example, the crosscorrelation for $n = -1, \sigma_2 = 2$ is improved from 0.58 for ZA to 0.86 for TZA, with a similar improvement in visual appearance (numbers quoted for $k_{nl} = 4k_f$). We therefore will compare statistics for nbody, FFA, and TZA; and the crosscorrelations of the latter two with nbody will be compared.

4. RESULTS

In Figures 1–4 we can see the qualitative, visual effect of the approximation. These plots are greyscale renderings of the mass density in slices from the nbody simulations, the FFA, and the TZA approximate solutions to the same initial conditions.

Generally speaking, the patterns all look quite similar for $n = -2$, Figure 4. However, the FFA looks as if the flow were held back a bit. This tendency to incomplete collapse is not serious here, but gets worse for more positive n. For $n = +1$, Figure 1, the FFA appears to consist of many more very small condensations than does the nbody simulation. The patterns appear to have very little in common. Figures 1–4 (c), the TZA, seems to have more resemblance to the nbody simulation, since the major condensations are of about the same size in the right place. TZA does seem to miss the small mass concentrations for the more positive spectra, and it connects the larger ones by spurious pancake–like bridges. These bridges contain very very little mass, however.

The results of our crosscorrelation analysis are given in Figure 5. Basically, two general results can be stated: (1) FFA performs better on an absolute scale as n decreases, and (2) TZA always performs better than FFA. These statements are in agreement with the visual impression. It is worth mentioning at this time that FFA performs better than ordinary ZA for the spectra $n = 0$ and $n = +1$ in terms of crosscorrelation analysis. Other workers (eg Brainerd et al. 1993, Bagla & Padmanabhan 1993) have compared their approximations to ZA. We have not done this for the reason that it is not difficult to outperform ZA for positive spectra, since it performs so badly (see CMS). So far TZA appears to be the standard to beat.

The power spectra of the evolved distributions are plotted in Figure 6. The results can be summarized easily. FFA underestimates small-k power for all initial conditions, and TZA is always quite good for small-k power, agreeing rather well up to about $0.6k_{nl}$.

Both approximations underestimate large-k power for all initial conditions, but FFA is always better than TZA. This appears to be the reason that FFA does succeed in making many small dense condensations. The normalization used here is one in which a Poisson distribution with 128^3 particles would produce, on average, $P = 1$.

A clue to the low crosscorrelation is present in Figure 7, where we plot $\langle \cos \theta \rangle$, where θ is the difference in phase angle between a given Fourier component in the result of the nbody simulation and that in its two approximate analogs. Of course 1 indicates perfect agreement, and 0 total randomization. For all spectra the phase agreement is much better for TZA than for FFA. MPS found in their experiments on the effects of various windows for TZA that all windows produced similar spectra in the results, but the phase agreement varied greatly, producing rather different crosscorrelations.

The integrated mass density distribution function $F(> \rho)$ (with clouds–in–cells binning of 128^3 particles on our 64^3 mesh) is plotted in Figure 8, and confirms some of our suspicions. In all cases except $n = +1$, FFA reproduces a more peaked density distribution than TZA so that more pixels reach high densities. Neither FFA nor TZA really produce a satisfactory fit, except at moderate δ for $n = -2$, but the FFA appears to be better overall. This is also the trend shown by the moment analysis of counts–in–cells at the same scale (e.g. Lucchin et al. 1993, for a wider introduction to this test); values for the variance, $\langle \delta^2 \rangle$, skewness $\langle \delta^3 \rangle$ (after shot–noise subtraction), for FFA, TZA and nbody simulations, are reported in Table 1.

5. DISCUSSION

In summary, the FFA does not seem able to reproduce the dynamics, in the sense of moving mass to the right places, at least for initial conditions with substantial power on small scales. The very simple TZA seems to work better in this respect. However, the FFA does succeed in producing small mass condensations, the major point of failure of TZA; but it does not seem to put them in the right place. Small–k power grows too slowly, and large–k power grows more correctly but with the wrong phases. This is probably because of the way dynamics acts in FFA: particles move along the initial streamlines to form "first generation" pancakes, filaments and knots, but no merging of these initial structures is allowed at all. Once the particles have come close to these structures, all of the later clustering evolution consists of the slow asymptotic fall of particles towards the wells of the initial gravitational potential. No structures on larger scales will ever form. Thus, it is not surprise that FFA provides better dynamical description in models with higher large–scale power, where the first formed pancakes and filaments already provide the large–scale structures. This is however an interesting feature, as the most popular cosmological scenarios (such as cold or hot dark matter) have low small–scale power. Also, FFA gives a better performance if evolved for less expansion factors (as in $n = -2, -1$ models here), as otherwise the large–scale pattern would significantly deviate both from nbody and linear theory. We suspect that a similar trend would arise in the LEP approximation, in spite of the different behaviour of particle trajectories near caustics (e.g. Bagla & Padmanabhan 1993). In order to improve the dynamical performance of these approximations one would probably need either initial small–scale smoothing or some account of the actual evolution of the velocity potential beyond linear theory. Improvements of FFA along these lines will

be discussed elsewhere. The good statistical performance of FFA is not in contradiction with the picture above. FFA seems to produce enough (or even too much) small–scale structure: cell count statistics on a given scale will generally show the correct trend, being only sensitive to the number of cells with the right occupation frequency, not to their exact location.

Future work will involve tests of the adhesion approximation (Shandarin & Zeldovich 1989), the Linear Evolution of Potential approximation (Brainerd et al. 1993; see also Bagla & Padmanabhan 1993), and higher order Zeldovich-like solutions (Buchert 1993 and references therein). It will be interesting to see whether any of the proposed improvements really go beyond the accuracy of the Zeldovich approximation, with truncation of modes that are too nonlinear to follow. So far, that 1970 proposal, with Gaussian filtering of modes that will act as noise, appears remarkably robust.

ACKNOWLEDGEMENTS

ALM gratefully acknowledges financial support from NSF grants AST–9021414, OSR–9255223, NASA Grant NAGW–2923, and computing support from the National Center for Supercomputing Applications, Urbana, Illinois, USA. FL, SM and LM acknowledge the Italian MURST for partial financial support, and the CINECA Computer Center (Bologna, Italy) for the use of computing facilities.

REFERENCES

Bagla J.S., Padmanabhan T., 1993, MNRAS, in press
Brainerd T.G., Scherrer R.J., Villumsen J.V., 1993, ApJ, in press
Buchert T., 1993, MNRAS, submitted
Coles P., Melott A.L., Shandarin S.F., 1993, MNRAS, 260, 765 (CMS)
Lucchin F., Matarrese S., Melott A.L., Moscardini L., 1993, ApJ, in press
Matarrese S., Lucchin F., Moscardini L., Saez D., 1992, MNRAS, 259, 437 (MLMS)
Melott A.L., Einasto J., Saar E., Suisalu I., Klypin A., Shandarin S.F., 1983, Phys. Rev. Lett., 51, 935
Melott A.L., Pellman T.F, Shandarin S.F., 1993, MNRAS, submitted (MPS)
Melott A.L., Shandarin S.F., 1993, ApJ, 410, 469 (MS)
Shandarin S.F., Zel'dovich Ya.B., 1989, Rev. Mod. Phys., 61, 185
Zel'dovich Ya.B., 1970, A&A., 5, 84

Figure captions

Figure 1. A greyscale plot of thin (L/128) slices of the simulation cube, and the approximations to it for index $n = +1$ initial conditions at the stage $k_{nl} = 8k_f$. (a) the nbody simulation (b) the frozen–flow approximation FFA (c) the Gaussian–truncated TZA model.

Figure 2. As in Figure 1, but for $n = 0$ initial conditions.

Figure 3. As in Figure 1, but for $n = -1$ initial conditions.

Figure 4. As in Figure 1, but for $n = -2$ initial conditions.

Figure 5. A plot of the crosscorrelation S as defined in the text between the density field generated by the full nbody simulations and the approximations versus the rms density fluctuation in the simulation. Both are smoothed by the same Gaussian window and refer to $k_{nl} = 8k_f$. Solid line: the frozen–flow approximation, FFA. Dashed line: the Gaussian–truncated TZA model.

Figure 6. Power spectra at $k_{nl} = 8k_f$ for the nbody simulations (dotted–dashed line), for FFA (solid line) and for Gaussian TZA (dashed line).

Figure 7. The average effective phase angle error, measured by ⟨cos Solid line: the frozen–flow approximation, FFA. Dashed line: the Gaussian–truncated TZA model.

Figure 8. The cumulative mass density distribution $F(> \rho)$ in terms of the number of cells with given density ρ, in units of the mean density, with clouds–in–cells binning of 128^3 particles on our 64^3 mesh.

Table 1. Moments of the density distribution.

variance

	nbody	FFA	TZA
$n = +1$	9.6	1.7	1.8
$n = 0$	9.3	3.3	1.9
$n = -1$	8.3	4.1	1.5
$n = -2$	8.5	3.2	2.6

skewness

	nbody	FFA	TZA
$n = +1$	240	7	10
$n = 0$	279	28	11
$n = -1$	298	47	11
$n = -2$	455	38	26

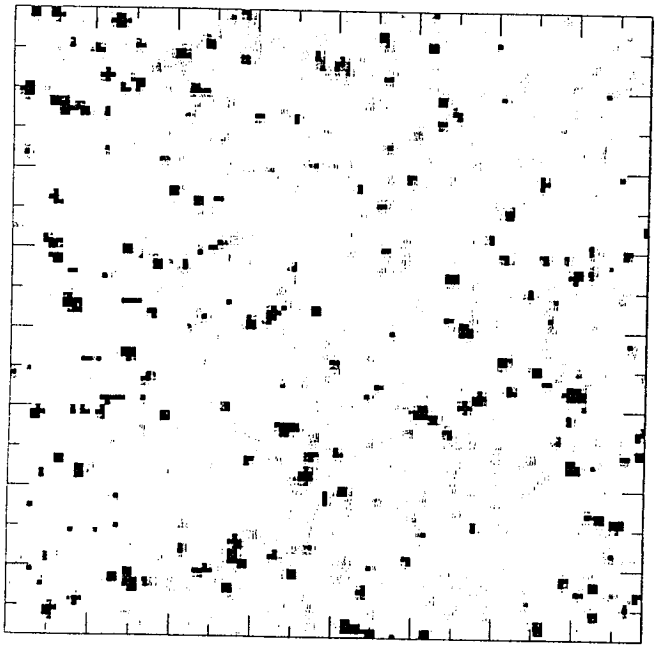

Fig 1a

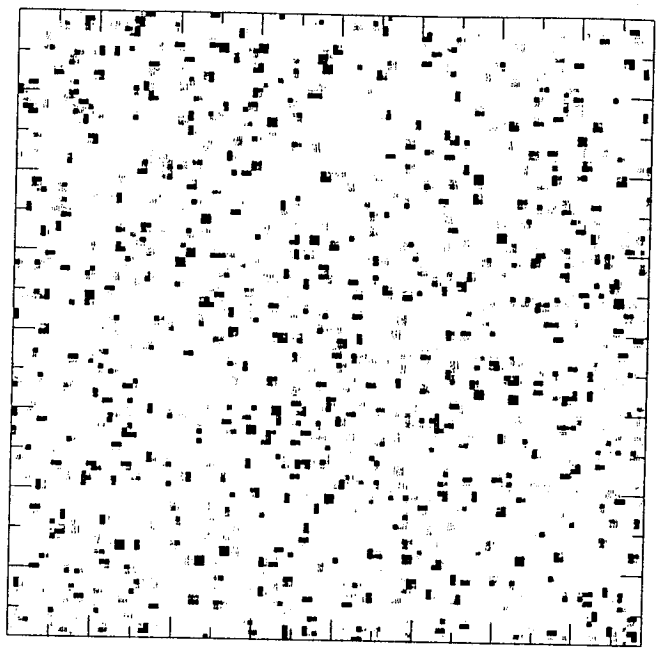

1b

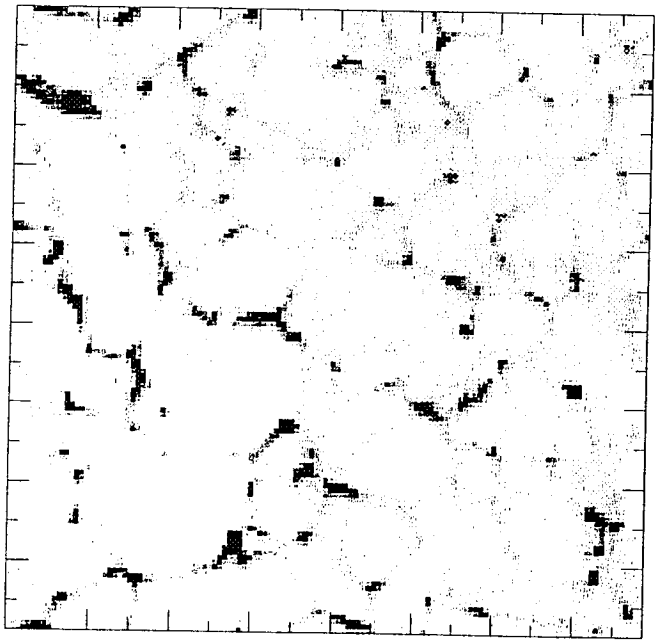

1c

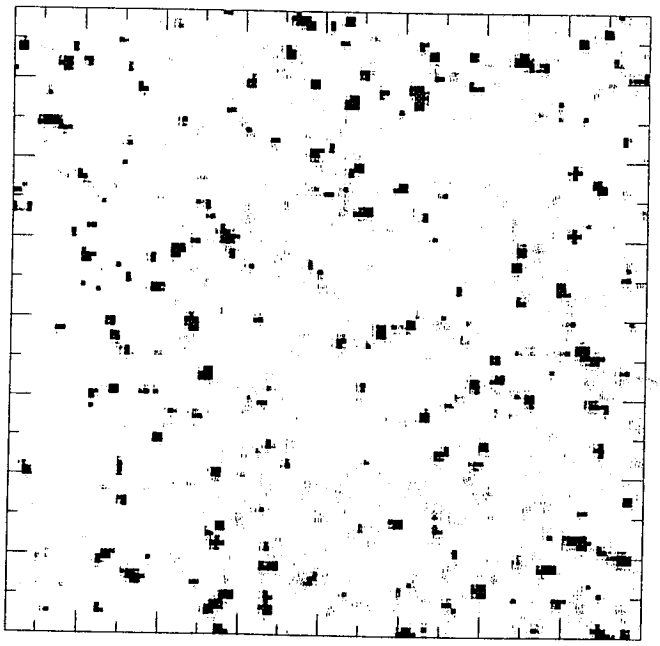

Fig 2a

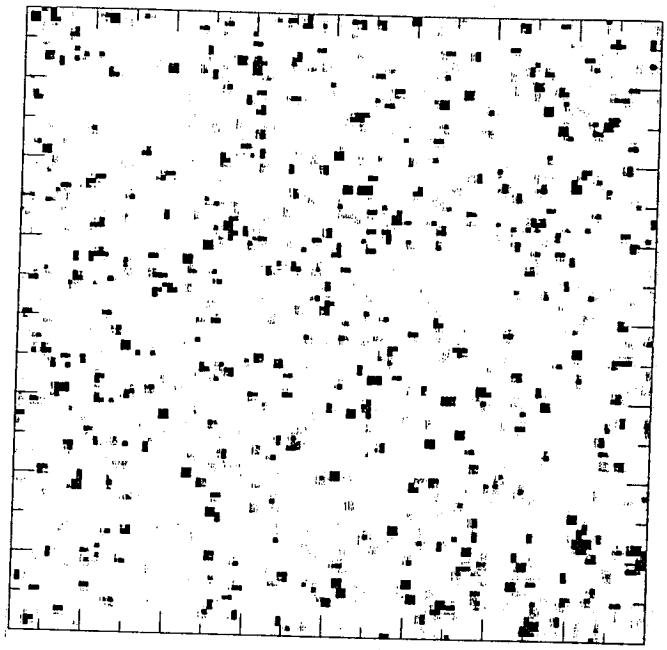

2b

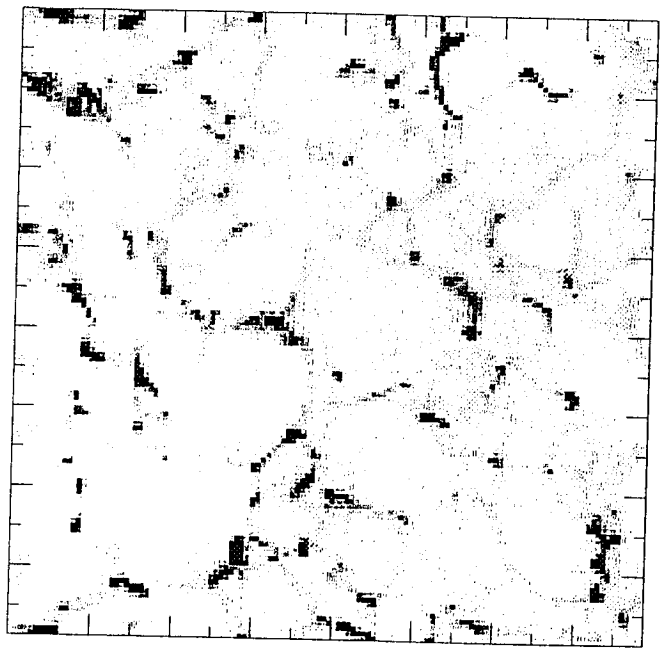

2c

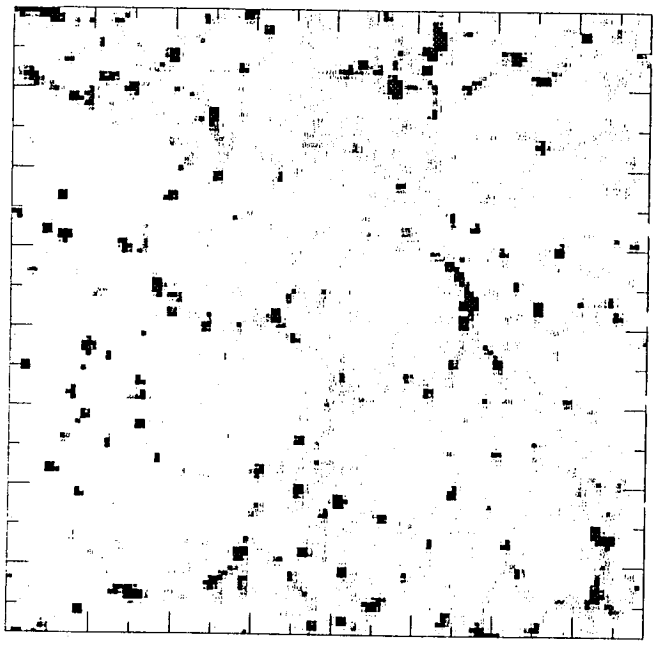

Fig 3a

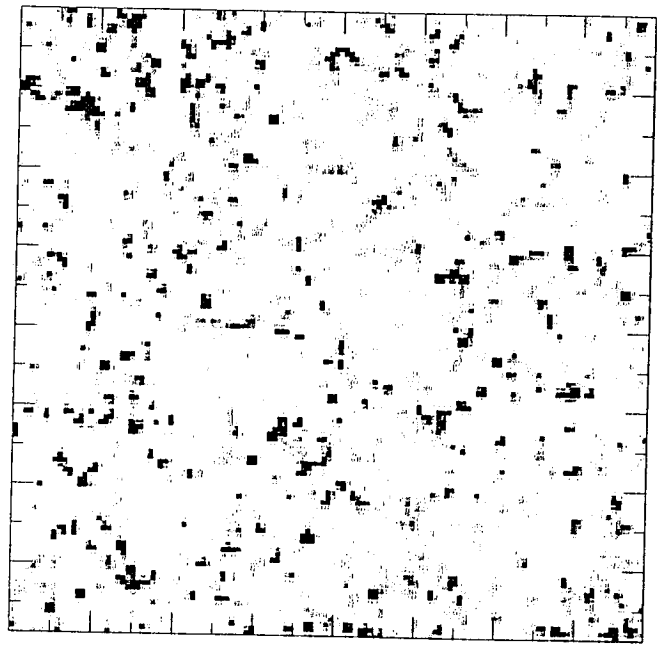

3b

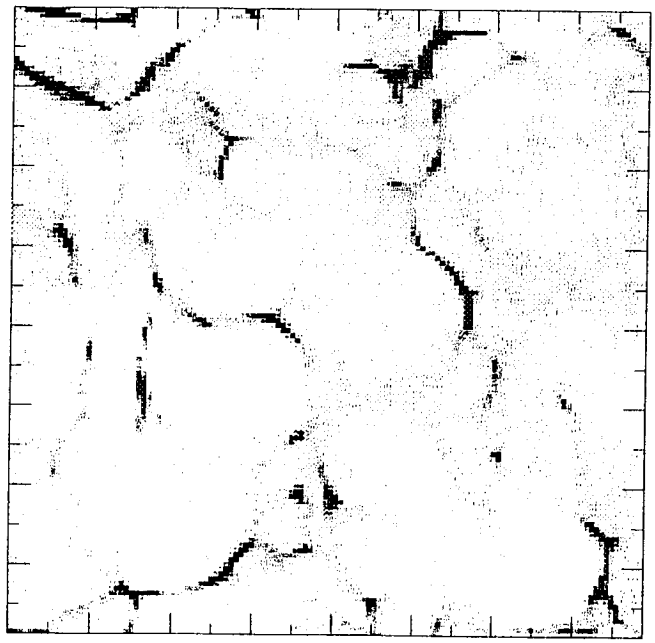

3c

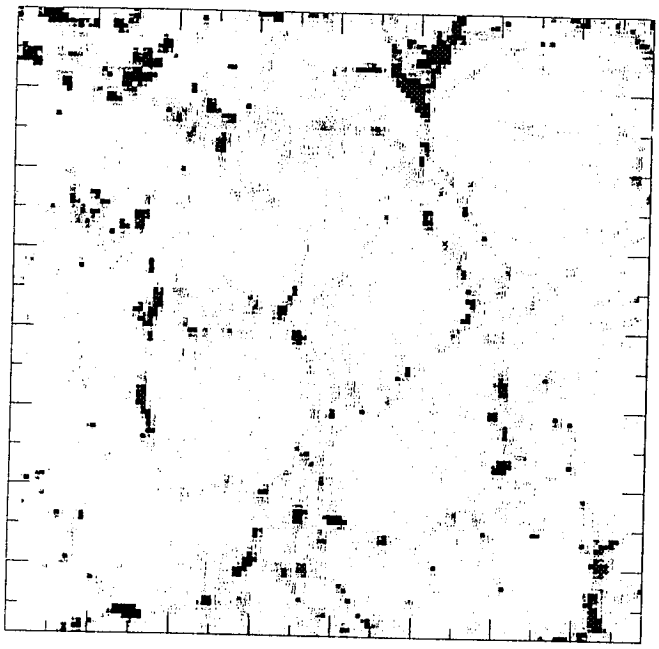

Fig 4a

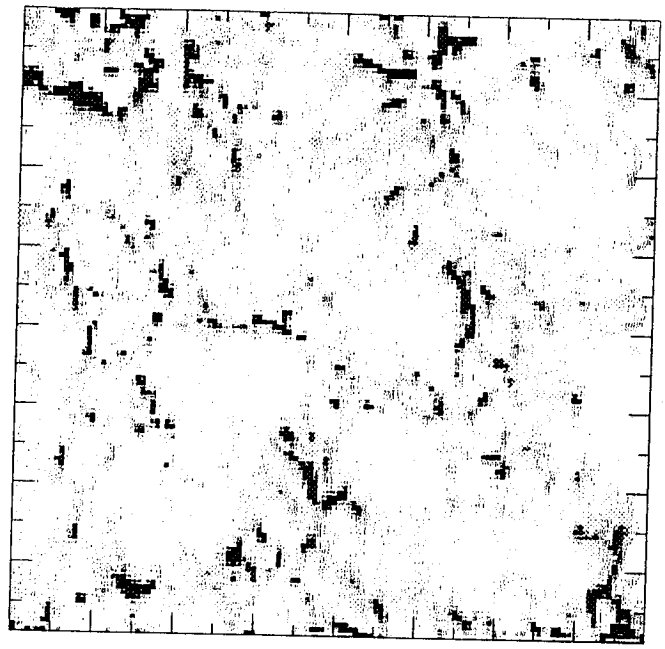

4b

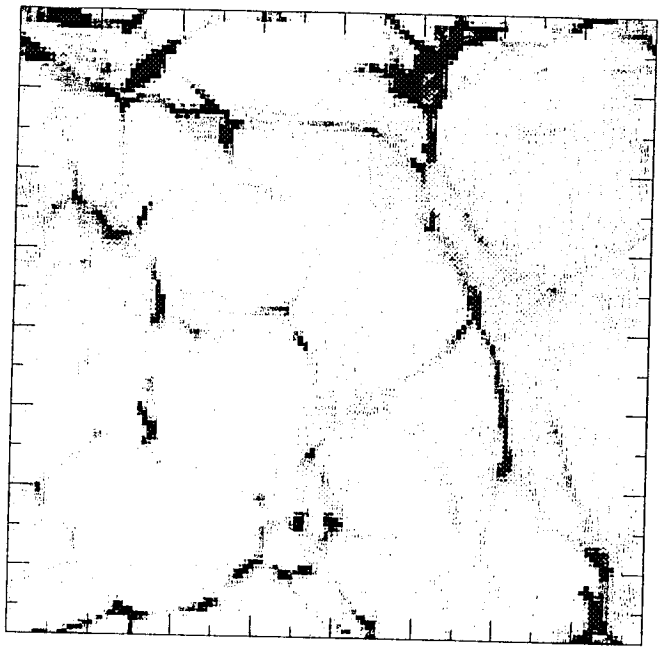

4c

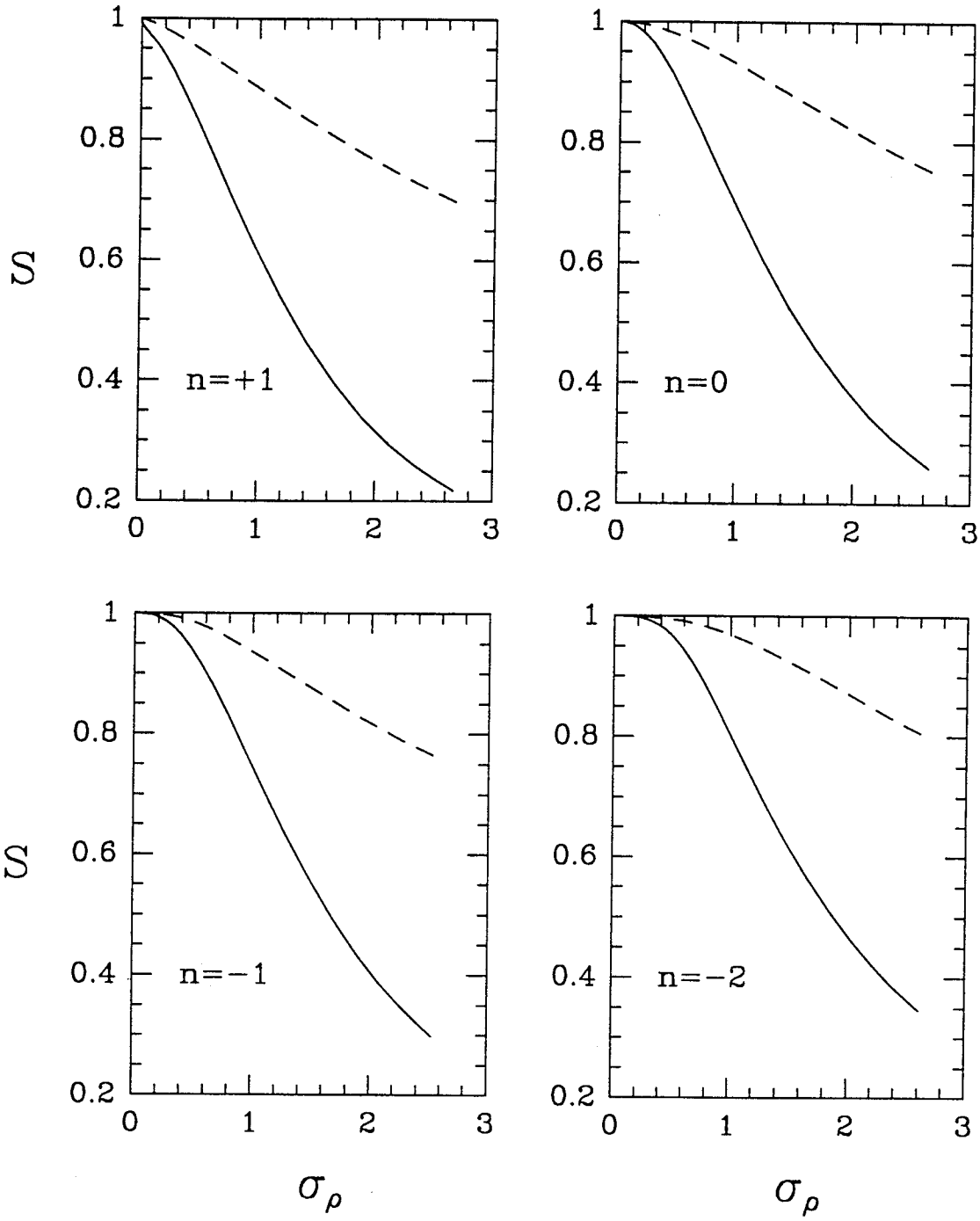

Fig 5

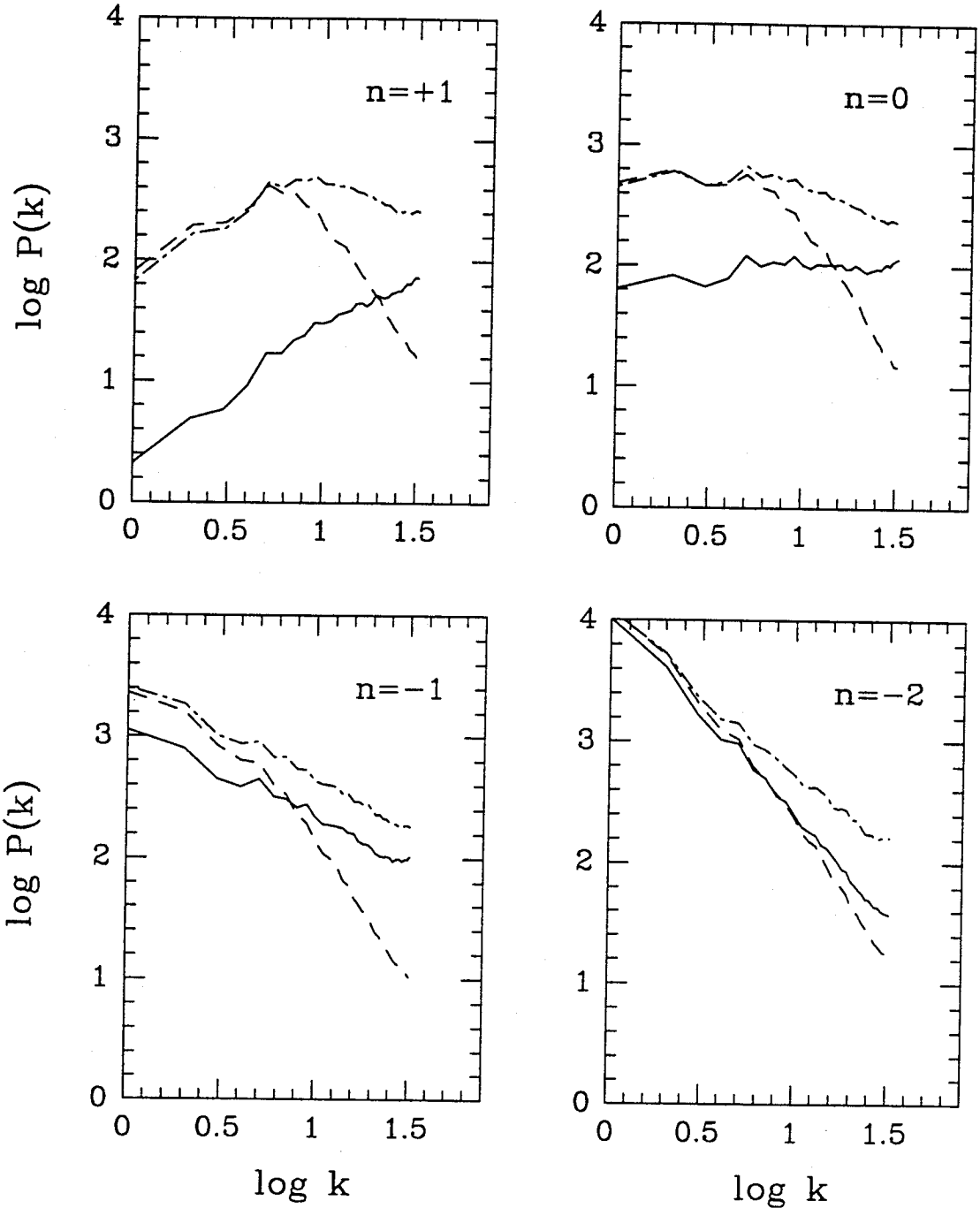

Fig 6

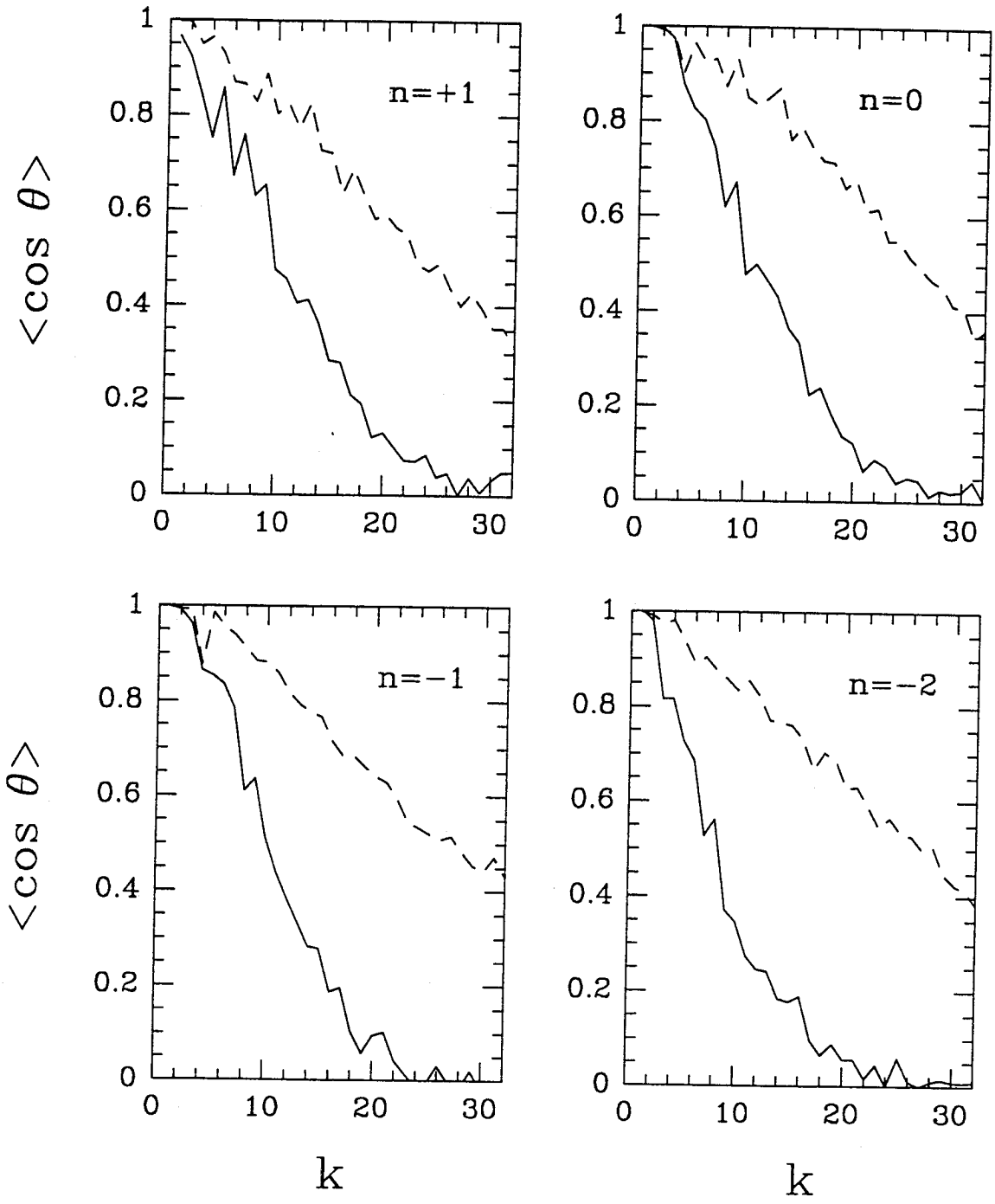

Fig 7

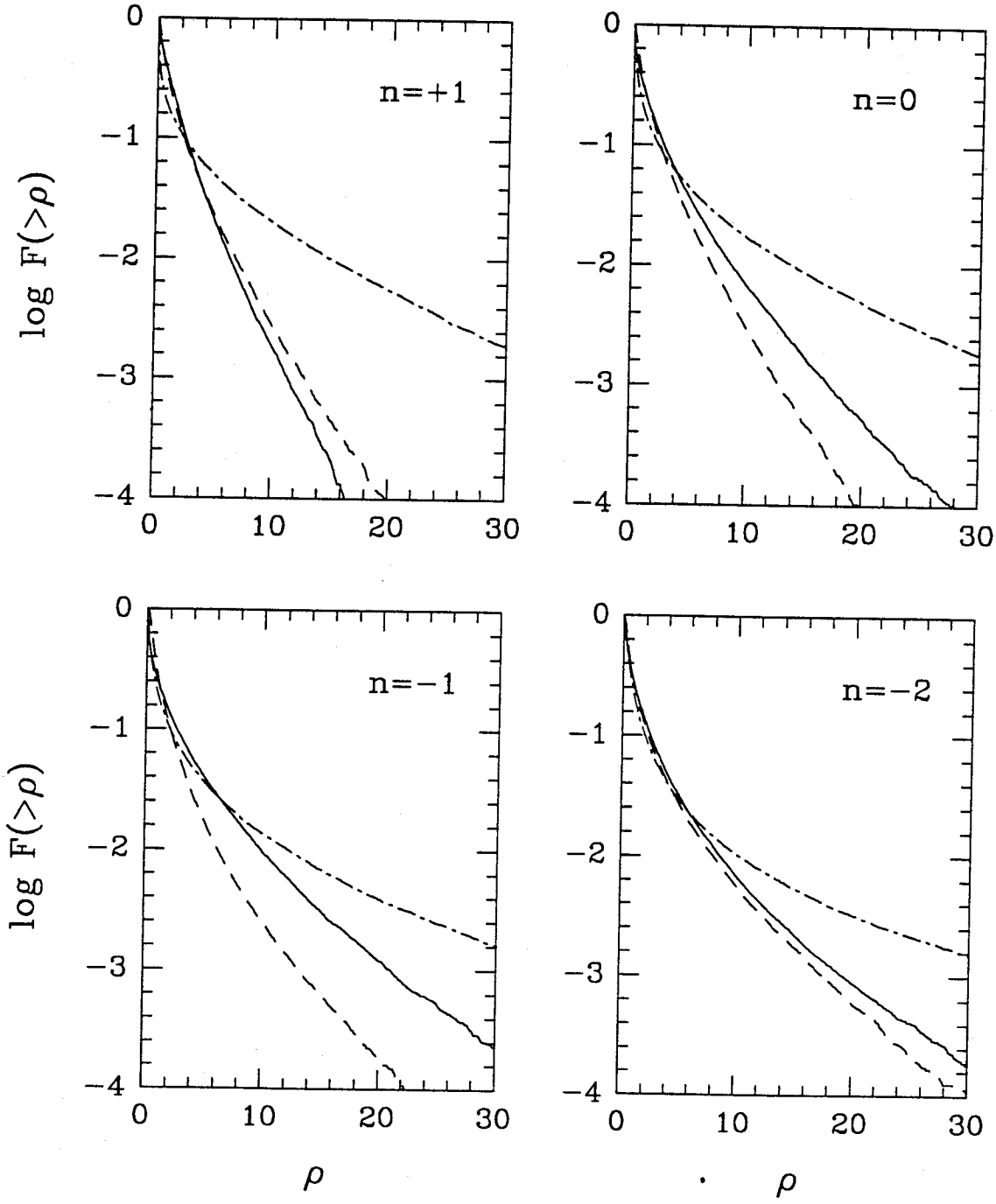

Fig 8